JOURNAL OF SOLID STATE CHEMISTRY 39, 351–359 (1981)

Electrical Conductivity in Strontium Titanate

U. BALACHANDRAN AND N. G. EROR*

Oregon Graduate Center, Beaverton, Oregon 97006

Received February 16, 1981; in final form May 18, 1981

The electrical conductivity of polycrystalline $SrTiO_3$ was determined for the oxygen partial pressure range of 10^0 to 10^{-22} atm and temperature range of 800 to 1050°C. The data were found to be proportional to the $-1/6$th power of the oxygen partial pressure for the oxygen pressure range 10^{-15}–10^{-22} atm, proportional to $P_{O_2}^{-1/4}$ for the oxygen pressure range 10^{-8}–10^{-15} atm, and proportional to $P_{O_2}^{+1/4}$ for the oxygen pressure range 10^0–10^{-3} atm. These data are consistent with the presence of very small amounts of acceptor impurities in $SrTiO_3$.

Introduction

Strontium titanate is one of the few titanium compounds which is cubic at room temperature. It has the perovskite structure. The electrical transport properties of semiconducting n-type $SrTiO_3$ were first investigated by Frederikse *et al.* (*1*), who found a band-type conduction process with an electron effective mass much greater than the free-electron mass and low-temperature mobilities greater than 1000 cm^2/V-sec. A theoretical examination of the electronic energy bands of strontium titanate has been carried out by Kahn and Leyendecker (*2*). Their calculations led to filled valence bands derived primarily from oxygen 2*p* orbitals and empty conduction bands derived predominantly from titanium 3*d* orbitals. From the optical transmission studies on single-crystal strontium titanate which was heated in vacuum, Gandy (*3*) determined an energy band of 3.15 eV. The oxygen self-diffusion has been studied by Paladino *et al.* (*4*) in single-crystal $SrTiO_3$. Walters and Grace (*5*) investigated the diffusion of point defects in $SrTiO_3$. Paladino (*6*) studied the oxidation kinetics of single-crystal $SrTiO_3$. On the basis of the oxygen self-diffusion and oxidation measurements, Paladino (*4, 6*) concluded that an oxygen vacancy defect model was applicable to $SrTiO_3$ at elevated temperatures.

Walters and Grace (*7*) examined the electrical conductivity and Seebeck coefficient of $SrTiO_3$ in water–hydrogen atmospheres for a narrow range of oxygen partial pressure. They also concluded that an oxygen vacancy model was applicable to their results. Yamada and Miller (*8*) have determined the carrier concentration by Hall effect measurements for single-crystal $SrTiO_3$ quenched from equilibrium with various oxygen partial pressures. All of the reported studies on $SrTiO_3$ indicate that there is an extensive range at low oxygen partial pressures (P_{O_2}), where the conductivity increases with decreasing P_{O_2}, characteristic of n-type conduction related to oxygen deficiency. The structural analog $BaTiO_3$ has been studied in much detail in both the polycrystalline (*9–14*) and single-crystal (*15*) states. These studies indicate that in the P_{O_2} range near 1 atm, the con-

* To whom correspondence should be addressed.

0022-4596/81/120351-09$02.00/0

ductivity increases with increasing P_{O_2}, characteristic of p-type conduction, related to a stoichiometric excess of oxygen. $SrTiO_3$, however, has not been studied in the past while in equilibrium with P_{O_2} near 1 atm, and no equilibrium behavior characteristic of p-type conduction has been reported.

In the present study, the high-temperature equilibrium electrical conductivity of polycrystalline $SrTiO_3$ prepared by the liquid mix technique has been measured. By matching the observed electrical characteristics to specific defect models the predominant defect structures are identified.

Experimental

The specimens employed in this investigation were prepared by a liquid mix technique (*16, 17*). Required amounts of strontium carbonate [Johnson-Mathey Corp., spec. pure], and tetraisopropyl titanate solution [Dupont Co., Tyzor] were dissolved in an ethylene glycol–citric acid solution. There was no evidence of any precipitation in the solutions as they were evaporated to a rigid transparent, uniformly colored polymeric glass. The glass retains homogeneity on an atomic scale and was calcined at 700–900°C—there was no evidence of a second phase in the as calcined samples. These powder samples were pressed into thin rectangular slabs [2.1 cm × 0.6 cm × .05 cm] under a load of 40,000 psi, and sintered in air at 1350°C for 12 hr. The density of the sintered slabs was 96% of the theoretical density. Conductivity specimens were cut from this sintered slab using an airbrasive unit. The specimens were wrapped with four 0.01-in. platinum wires as described in the literature (*18, 19*). Small notches were cut in the edges of the sample to aid in holding the platinum wires in place.

A conventional four-probe direct current technique was employed for all electrical conductivity measurements. The four platinum leads were insulated from one another by recrystallized high-purity alumina insulators. A standard taper Pyrex joint to which capillary tubes had been sealed was mounted on top of the furnace reaction tube assembly. The platinum wires exited through the capillary tubes and were glass sealed vacuum tight into the tubes.

The oxygen partial pressures surrounding the samples were controlled by flowing metered mixtures of gases past the sample. The gases were oxygen, air plus argon, argon with known amounts of oxygen and CO_2/CO mixtures. The error in volumetric ratio measurements of CO_2/CO gas mixtures resulted in an error of about 1% in the P_{O_2} value reported here. The conductivity was measured as a function of P_{O_2} in the temperature range 800–1050°C. The conductivity was determined by measuring the voltage across the potential probes using a high-impedance [$<10^{10}$ ohm] digital voltmeter [Keithley 191 Digital Multimeter]. The current was supplied between the two outer leads by a constant-current source [Keithley 225 current source]. The voltage was measured with the current in both forward and reverse directions, and the conductivity was calculated from the average values. Current was varied from 20 μA to 1 mA and no significant change in conductivity was observed.

Results

The electrical conductivity of polycrystalline $SrTiO_3$ in the temperature range 800–1050°C and in equilibrium with oxygen partial pressures between 10^{-22} and 10^{-15} atm is shown in Fig. 1. The slopes of the straight lines ($-\frac{1}{6}$) drawn through the data are given in Table I. Table II gives the activation enthalpy for conduction in this region. Figure 2 shows the temperature dependence of the conductivity for eight selected P_{O_2} values. The log σ vs log P_{O_2} and the temperature dependence of con-

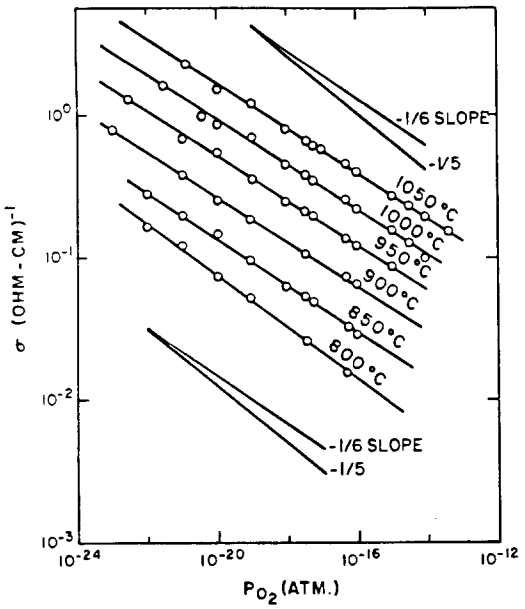

FIG. 1. The conductivity of polycrystalline $SrTiO_3$ as a function of oxygen partial pressure at constant temperature, from 10^{-22} to 10^{-15} atm.

ductivity in the P_{O_2} range 10^{-15}–10^{-8} atm are shown in Figs. 3 and 4, respectively. The activation enthalpy for conduction in this range of P_{O_2} is given in Table III. Figures 6 and 7 show the variation of electrical conductivity with oxygen partial pressure and temperature respectively for the $P_{O_2} > 10^{-6}$ atm. The slopes of the linear part in Fig. 6 and the activation enthalpy from the Arrhenius slopes are given in Table IV and Table V, respectively. An Arrhenius plot of the conductivity minima (σ_{min}) is given in Fig. 5.

TABLE I

P_{O_2} DEPENDENCE OF CONDUCTIVITY IN THE REGION 10^{-22}–10^{-15} atm

T (°C)	m for $\sigma_n \propto P_{O_2}^{-1/m}$
800	5.5
850	6.06
900	6.3
950	6.3
1000	6.3
1050	6.3

TABLE II

ACTIVATION ENTHALPIES FOR CONDUCTION IN THE REGION 10^{-22}–10^{-15} atm

P_{O_2} (atm)	Activation enthalpies [kcal/mole]
10^{-22}	110.61
10^{-21}	109.72
10^{-20}	110.67
9.3×10^{-20}	111.17
10^{-18}	110.98
10^{-17}	112.68
5×10^{-17}	114.67
5×10^{-16}	113.88

Discussion

Region I: [$P_{O_2} = 10^{-2}$–10^{-15} *atm*]

The log σ vs log P_{O_2} data [Fig. 1] are linear for as many as seven decades of oxygen partial pressure for a given temper-

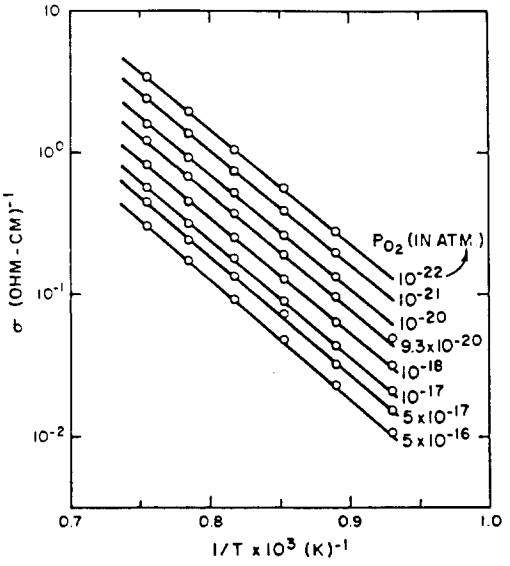

FIG. 2. Temperature dependence of conductivity of polycrystalline $SrTiO_3$ in the n-type, oxygen-deficient region.

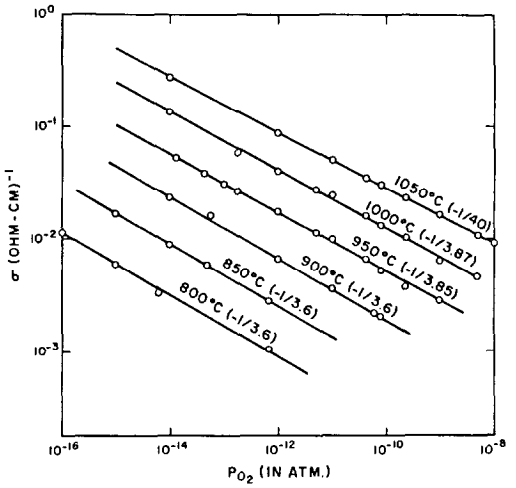

FIG. 3. The conductivity of polycrystalline $SrTiO_3$ as a function of oxygen partial pressure at constant temperature, from 10^{-15} to 10^{-8} atm.

TABLE III

ACTIVATION ENTHALPIES FOR CONDUCTION IN THE REGION 10^{-15}–10^{-8} atm

P_{O_2} (atm)	Activation enthalpies [kcal/mole]
10^{-15}	100.70
10^{-14}	100.62
10^{-13}	102.42
10^{-12}	104.02
10^{-11}	103.71
10^{-10}	112.34
10^{-9}	112.66

TABLE IV

P_{O_2} DEPENDENCE OF CONDUCTIVITY FOR THE p-TYPE REGION

T (°C)	m for $\sigma_p \propto P_{O_2}^{1/m}$
800	4.08
850	4.3
900	4.2
950	4.2
1000	4.6
1050	4.6

TABLE V

ACTIVATION ENTHALPIES FOR CONDUCTION IN THE p-TYPE REGION

P_{O_2} (atm)	Activation enthalpies [kcal/mole]
10^{0}	34.72
5×10^{-1}	34.32
2.1×10^{-1}	35.10
10^{-1}	34.60
1.8×10^{-2}	39.20
1×10^{-2}	37.30
4.48×10^{-3}	39.80
5×10^{-4}	38.52

ature. This extensive region of linearity affords the opportunity to determine the defect model responsible for the n-type electrical conductivity in this region. A slope of approximately $-\frac{1}{6}$ is found for the $\log \sigma$ vs $\log P_{O_2}$ data. This slope is similar to that found for $BaTiO_3$ (*12–15*) and $CaTiO_3$ (*20*) as well as the results of Walters and Grace (*7*) for single-crystal $SrTiO_3$ in the

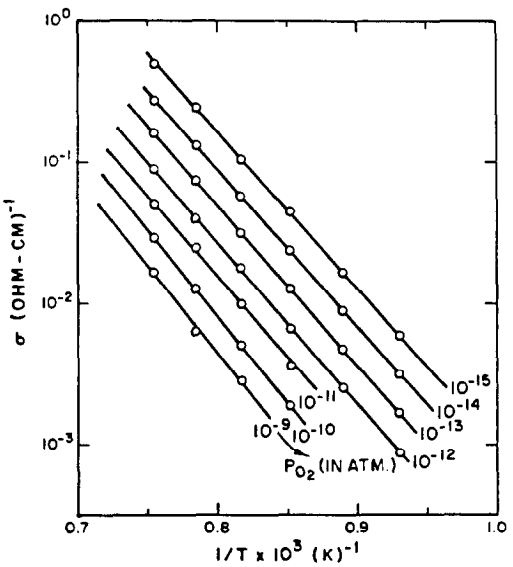

FIG. 4. Temperature dependence of conductivity of polycrystalline $SrTiO_3$ in the n-type, oxygen-deficient region.

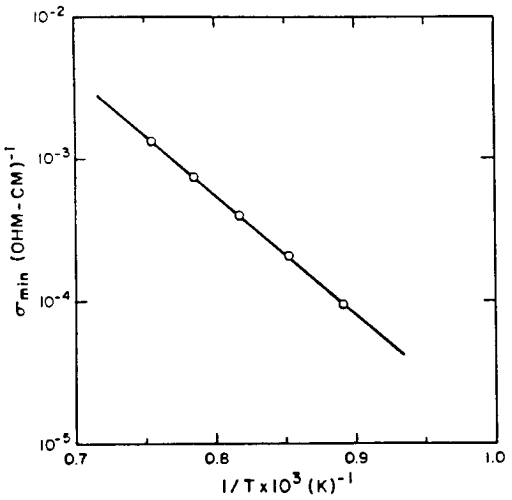

FIG. 5. Temperature dependence of the conductivity minimum of polycrystalline $SrTiO_3$.

narrow P_{O_2} range [10^{-21}–10^{-19} atm]. Yamada and Miller (*8*) have determined the carrier concentration by Hall effect measurements for single-crystal $SrTiO_3$ quenched from equilibrium with various oxygen partial pressures, and they found a similar relationship between the electron concentration and the equilibrium partial pressure. These same authors have shown that the oxygen vacancies formed upon reduction can be quenched-in upon cooling to ambient and they remain doubly ionized to very low temperatures.

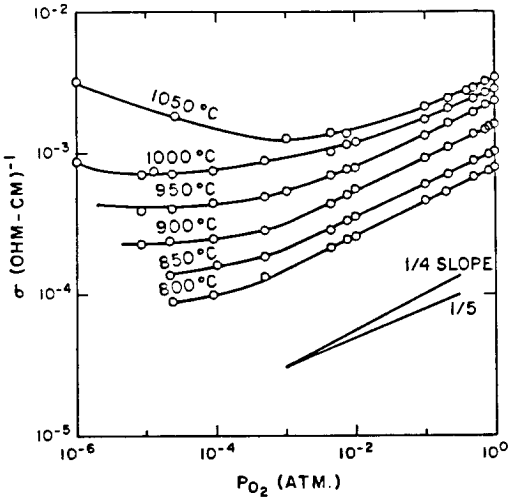

FIG. 6. The conductivity of polycrystalline $SrTiO_3$ as a function of oxygen partial pressure at constant temperature, from 10^{-8} to 10^{0} atm.

The variation of the electrical conductivity with the oxygen partial pressure is calculated in terms of the oxygen vacancy defect model. The basis for the calculation is the reaction that represents the formation of a doubly ionized oxygen vacancy [$V_{\ddot{O}}$] and two electrons available for conduction by the removal of an oxygen from a normal lattice site into the gas phase. The reaction is

$$O_O \rightleftharpoons \tfrac{1}{2}O_2 + V_{\ddot{O}} + 2e'. \qquad (1)$$

The equilibrium constant for the reaction (1) is

$$K_1 \cong [V_{\ddot{O}}][n]^2 P_{O_2}^{1/2} = \exp\left(\frac{-\Delta G_f}{RT}\right), \qquad (2)$$

where $[n] \equiv e'$. It is assumed that the defects exist in a dilute solution and do not interact. The Gibbs standard free energy change for reaction (1) is represented by ΔG_f. With two electrons resulting from each oxygen vacancy it follows that

$$[n] \cong 2[V_{\ddot{O}}]. \qquad (3)$$

Expressing the free energy change in terms of the enthalpy change, ΔH_f, and entropy change ΔS_f and substituting Eq. (3) into Eq. (2) the result for the electron concentration is

$$[n] = 2^{1/3} P_{O_2}^{-1/6} \exp\left[\frac{\Delta S_f}{3R}\right] \exp\left[\frac{-\Delta H_f}{3RT}\right]. \qquad (4)$$

The electrical conductivity, σ, for the case where the sole charge carriers are electrons in the conduction band is

$$\sigma = ne\mu, \qquad (5)$$

where e is the electronic charge, and μ is the mobility of the conduction electrons. When Eq. (4) is substituted into Eq. (5), the electrical conductivity becomes

$$\sigma = 2^{1/3}P_{O_2}^{-1/6}e\mu \exp\left[\frac{\Delta S_f}{3R}\right]\exp\left[\frac{-\Delta H_f}{3RT}\right]. \quad (6)$$

At constant temperature, assuming that mobility is independent of the change in concentration of oxygen vacancies, a plot of the logarithm of the electrical conductivity vs the logarithm of the P_{O_2} should result in a straight line with a slope of $-\frac{1}{6}$. The data in Fig. 1 and Table I are in good agreement with the predicted $-\frac{1}{6}$ dependence.

An indication of the magnitude of ΔH_f, the enthalpy of the oxygen extraction reaction, is typically obtained from Arrhenius plots of the conductivity, as deduced from Eq. (6). This procedure neglects contributions from the temperature dependences of the carrier mobility or density of states. The value of ΔH_f calculated from the slope of the Arrhenius plots in Fig. 2 are listed in Table I. An average value of 4.85 eV [111.8 kcal/mole] is estimated for ΔH_f. Walters and Grace (*7*) obtained a value of 6.3 eV. Yamada and Miller (*8*) determined a value for ΔH_f of 5.76 ± 0.2 eV for $SrTiO_3$. This was based on a direct measurement of n by the Hall effect on reduced single crystals.

The temperature dependence of mobility of electrons in $SrTiO_3$ is not known for the temperature range covered in the present study. Frederikse *et al.* (*1*) found a band-type conduction process in $SrTiO_3$. This implies that electron mobility varies proportional to $T^{-3/2}$ and the equilibrium constant K_1 in Eq. (2) should thus contain N_c^2, the square of the density of states near the conduction band edge. For $\mu_n \propto T^{-3/2}$ and $N_c \propto T^{3/2}$ there is an additive correction to ΔH_f of $3/2RT$-RT or about 0.11 eV. Seuter (*13*) has determined the mobility of electrons in $BaTiO_3$ in the temperature range 800–1000°C by a combination of the Hall effect and conductivity. He describes the temperature dependence as T^{-1}. If $\mu \propto T^{-1}$, then the corrections for ΔH_f cancel.

Region II [$P_{O_2} = 10^{-8}$–10^{-15} *atm*]

A slope of approximately $-\frac{1}{4}$ is found for the log σ vs log P_{O_2} data [see Fig. 3]. Daniels and Hardtl (*21*) reported from their log σ vs. log P_{O_2} plot, a slope of $-\frac{1}{4}$ between 700 and 900°C and $-\frac{1}{5}$ at 1200°C for $BaTiO_3$ in the P_{O_2} range, 10^{-18}–10^{-8} atm. They attributed the $-\frac{1}{4}$ slope to singly ionized oxygen vacancies as the cause of conductance and $-\frac{1}{5}$ value to the more frequent occurrence of doubly ionized oxygen vacancies. However, for $SrTiO_3$, it has been shown by earlier investigators (*5, 8*), that the oxygen vacancies of the quenched samples remain doubly ionized down to liquid nitrogen temperature. The observed slope of $-\frac{1}{4}$ in this region must, therefore, be due to the presence of an unknown, negatively charged impurity, i.e., an acceptor impurity such as Al, Fe, or Cr on Ti sites. For the case of undoped $BaTiO_3$ prepared by the same technique as the one used here, Chan and Smyth (*14*) report a net acceptor impurities about 130 ppm (atomic). They proposed that all undoped material [$BaTiO_3$] studied to date had a net excess of acceptor impurities, and attributed this to the fact that potential acceptor elements are naturally much more abundant than potential donor elements. Seuter (*13*) was able to observe an extensive range of $P_{O_2}^{-1/4}$ dependence for conductivity in the oxygen-deficient region below the p–n transition in the $BaTiO_3$, presumably because of greater acceptor impurity content of his samples. We believe that our samples also contain some unknown acceptor impurities which are singly ionized. Thus the condition of charge neutrality in this region can be

$$2[V_{\ddot{O}}] \cong [A']. \quad (7)$$

With this neutrality condition and Eqs. (1), (2), (4), and (5), the conductivity varies with oxygen partial pressure as shown in Eq. (8) below.

$$\sigma = 2^{1/2}\frac{1}{[A']^{1/2}} P_{O_2}^{-1/4} e\mu \exp\left[\frac{\Delta S_f}{2R}\right]\exp\left[\frac{-\Delta H_f}{2RT}\right]. \quad (8)$$

The slopes of the lines drawn in Fig. 3 are in agreement with the predicted value of $-\frac{1}{4}$ by the above impurity model. The activation enthalpies of conduction derived from the Arrhenius slopes [see Fig. 4] are shown in Table III. An average value of 4.56 eV [105.2 kcal/mole] is estimated for this region.

Transition Region

Becker and Frederikse (*22*) showed that the band-gap energy (extrapolated to zero temperature) of a semiconductor which exhibits a p–n transition may be determined from the Arrhenius plots of the conductivity minima. The log σ_{min} vs $1/T$ data in Fig. 5 indicate a value E_g° = 3.36 eV [77.54 kcal/mole] as the band gap for the polycrystalline $SrTiO_3$ extrapolated to 0°K. This is in good agreement with the range of values 3.2–3.4 eV reported from optical absorption data (*23–25*) on single-crystalline $SrTiO_3$. Assuming band conduction for both electrons and holes, the full expression for the Arrhenius plot is

$$\frac{\partial \ln \sigma_{min}}{\partial (RT)^{-1}} = \frac{\partial}{\partial (RT)^{-1}}\left[\frac{\ln \mu_n \mu_p}{2} + \ln N_c N_v\right] - \frac{E_g^\circ}{2}. \quad (9)$$

Assuming that the temperature dependence of the mobilities is the same for electrons and holes, and if both N_c and N_v, the density of states near the valence band edge, are proportional to $T^{+3/2}$, mobility and density of states terms cancel each other, and the Arrhenius slope is directly proportional to E_g°.

Region III [$P_{O_2} > 10^{-3}$ *atm*]

The conductivity in this region increases with increasing oxygen partial pressure [see Fig. 6], indicative of p-type, or oxygen-excess, conductivity. The region of linearity in the p-type region increases in width with decreasing temperature as the p–n transition moves to lower P_{O_2}. The slopes of the pressure dependence given in Table IV indicate that the values are tending toward $\frac{1}{4}$ with decreasing temperature where the range of linearity is greatest. Measurements of the electrical conductivity under fixed oxygen pressure as a function of temperature result in a nearly constant value for the slopes of log σ vs $1/T$ for various oxygen partial pressures in this region [Fig. 7]. The activation enthalpies of conduction, ΔH_p, derived from the slopes are given in Table V. A value of about 1.59 eV [36.7 kcal/mole] appears to be typical.

It is apparent that a stoichiometric excess of oxygen can be incorporated into $SrTiO_3$ by a remarkably favorable process without the need of creating a crystallographic excess. The oxygen is incorporated into the impurity-related oxygen vacancies where

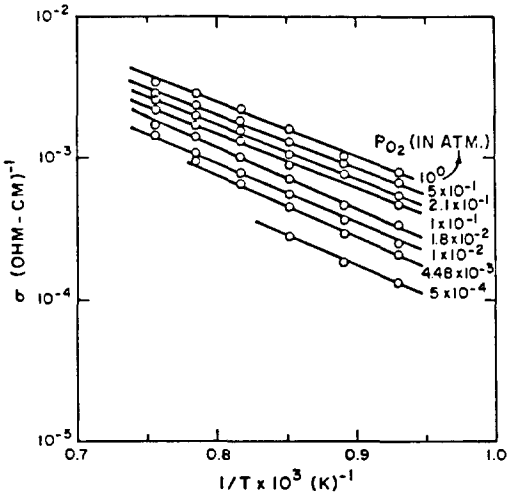

FIG. 7. Temperature dependence of conductivity of polycrystalline $SrTiO_3$, in the p-type region.

the reaction is,

$$[V_{\ddot{O}}] + \tfrac{1}{2}O_2 \rightleftharpoons O_O + 2h. \qquad (10)$$

The charge neutrality condition near the stoichiometric region is

$$[A'] \cong 2[V_{\ddot{O}}]. \qquad (11)$$

The chemical mass action expression for Eq. (10) combined with Eq. (11) gives

$$\sigma \propto P_{O_2}^{+1/4}, \qquad (12)$$

as observed, as long as only a minor fraction of the impurity-related $V_{\ddot{O}}$ is filled. If a significant proportion of the $V_{\ddot{O}}$ has been filled then both h and $V_{\ddot{O}}$ become dependent on P_{O_2}. The trend toward shallower slopes at higher temperatures represents an intrusion of the transition region leading to the conductivity minima which are moving toward higher P_{O_2} with increasing temperature. The ready availability of oxygen vacancies explains the unusual ease with which the material accepts a stoichiometric excess of oxygen.

Earlier investigators (*11, 14, 15*) have invoked the presence of an unknown acceptor impurities in order to explain their very similar experimental results in $BaTiO_3$ in the P_{O_2} range under consideration. The estimated acceptor impurity in our sample is approximately 170 ppm. These impurities and their charge compensating partner, $V_{\ddot{O}}$ dominate the charge neutrality condition in a wide range of P_{O_2} ($>10^{-15}$ atm). The only region where impurity-insensitive behavior is observed is in the range of lowest P_{O_2} and highest temperature where the conductivity varies as $P_{O_2}^{-1/6}$ and the $V_{\ddot{O}}$ generated by Eq. (1) exceed those due to the acceptor impurity.

When the conductivities obtained from this work are compared with the reported data of Walters and Grace (*7*) in the narrow range of P_{O_2} used by them, the two values are well within the range 0.03 ohm^{-1} cm^{-1}. This agreement between the polycrystalline sample used in this investigation and the single crystal used by Walters and Grace (*7*) indicates that grain boundaries have no significant effect on electronic transport in this range of experimental conditions.

Conclusions

The experimental results agree well with the predictions based on a doubly ionized oxygen vacancy defect model at the lowest P_{O_2} and temperature range 800–1050°C. The logarithm of the electrical conductivity is a linear function of the logarithm of P_{O_2} at constant temperature. A slope of $-\frac{1}{6}$ is observed in the region 10^{-22}–10^{-15} atm and this agrees with the predicted value.

For $P_{O_2} > 10^{-15}$ atm the defect chemistry of $SrTiO_3$ is dominated by accidental acceptor impurities and their related oxygen vacancies, Eq. (7). Because of these acceptor impurities, a region in which a $P_{O_2}^{-1/4}$ dependence for the conductivity is observed.

The p-type conductivity observed in the region $P_{O_2} > 10^{-3}$ atm results from a stoichiometric excess of oxygen which occupies the impurity-related oxygen vacancies, Eq. (10). Thus, a stoichiometric excess of oxygen is achieved even while not all of the available oxygen sites are occupied. The ready availability of oxygen vacancies results in low enthalpy for the oxygen incorporation reaction.

References

1. H. P. R. Frederikse, W. R. Thurber, and W. R. Hosler, *Phys. Rev. A* **134,** 442 (1964).
2. A. H. Kahn and A. J. Leyendecker, *Phys. Rev. A* **135,** 1321 (1964).
3. H. W. Gandy, *Phys. Rev.* **113,** 795 (1959).
4. A. E. Paladino, L. G. Rubin, and J. S. Waugh, *J. Phys. Chem. Solids* **26,** 391 (1965).
5. L. C. Walters and R. E. Grace, *J. Phys. Chem. Solids* **28,** 245 (1967).
6. A. E. Paladino, *Bull. Amer. Ceram. Soc.* **48,** 476 (1965).
7. L. C. Walters and R. E. Grace, *J. Phys. Chem. Solids* **28,** 239 (1967).

8. H. YAMADA AND G. R. MILLER, *J. Solid State Chem.* **6,** 169 (1973).
9. H. VEITH, *Z. Angew. Phys.* **20,** 16 (1965).
10. F. FOSEK AND H. AREND, *Phys. Status Solidi* **24,** K69 (1967).
11. S. A. LONG AND R. N. BLUMENTHAL, *J. Amer. Ceram. Soc.* **54,** 515 (1971).
12. S. A. LONG AND R. N. BLUMENTHAL, *J. Amer. Ceram. Soc.* **54,** 577 (1971).
13. A. M. J. H. SEUTER, *Philips Res. Rep. Suppl.* No. 3, 1 (1974).
14. N. H. CHAN AND D. M. SMYTH, *J. Electrochem. Soc.* **123,** 1585 (1976).
15. N. G. EROR AND D. M. SMYTH, *J. Solid State Chem.* **24,** 235 (1978).
16. M. PECHINI, U.S. Patent, 3,330,697, July 11, 1967.
17. N. G. EROR AND D. M. SMYTH, *in* "Chemistry of Extended Defects in Nonmetallic Solids" (L. Eyring and M. O'Keefe, Eds.), pp. 62–74. North-Holland, Amsterdam (1970).
18. S. P. MITOFF, *J. Chem. Phys.* **35,** 882 (1961).
19. J. B. PRICE AND J. B. WAGNER, *Z. Phys. Chem.* **49,** 257 (1966).
20. W. L. GEORGE AND R. E. GRACE, *J. Phys. Chem. Solids* **30,** 881 (1969).
21. J. DANIELS AND K. H. HARDTL, *Philips Res. Rep.* **31,** 489 (1976).
22. J. H. BECKER AND H. P. R. FREDERIKSE, *J. Appl. Phys.* **33,** 447 (1962).
23. T. A. NOLAND, *Phys. Rev.* **94,** 724 (1954).
24. M. CARDONA, *Phys. Rev. A* **140,** 651 (1965).
25. M. I. COHEN AND R. F. BLUNT, *Phys. Rev.* **168,** 929 (1968).